

The 3D Grazing Collision of Two Black Holes

Miguel Alcubierre⁽¹⁾, Werner Benger^(1,2), Bernd Brügmann⁽¹⁾, Gerd Lanfermann⁽¹⁾, Lars Nerger⁽¹⁾,
Edward Seidel^(1,3), and Ryoji Takahashi⁽¹⁾

⁽¹⁾ Max-Planck-Institut für Gravitationsphysik, Am Mühlenberg 1, D-14476 Golm, Germany

⁽²⁾ Konrad-Zuse-Zentrum für Informationstechnik Berlin, Takustrasse 7, D-14195 Berlin, Germany

⁽³⁾ National Center for Supercomputing Applications, Beckman Institute, 405 N. Mathews Ave., Urbana, IL 61801
(September 14, 2019; AEI-2000-080)

We present results for full 3D evolutions of two colliding black holes (BHs), with angular momentum, spin, and unequal mass. For the first time gravitational waveforms are computed for a grazing collision. The collision can be followed through the merger to form a single BH, and through part of the ringdown period of the final BH. The apparent horizon is tracked and studied, and physical parameters, such as the mass of the final BH, are computed. The total energy radiated in gravitational waves is shown to be consistent with the total mass of the spacetime and the final BH mass. The implication of these simulations for gravitational wave astronomy is discussed.

04.25.Dm, 04.30.Db, 97.60.Lf, 95.30.Sf

The collision of two black holes (BHs) is considered by many researchers to be a primary candidate for generating detectable gravitational waves, and hence is the focus of attention for many research groups worldwide. As the first generation of gravitational wave detectors [1], with enough sensitivity to potentially detect waves, is coming online for the first time within a year, the urgency of providing theoretical information needed not only to interpret, but also to detect the waves, is very high. However, even in axisymmetry, the problem has proven to be extremely difficult, requiring nearly 20 years to solve in even limited cases (e.g. [2–6]). In full 3D progress has been rather slow due to many factors, including (but not limited to) unexpected numerical instabilities, limited computer power, and the difficulties of dealing with spacetime singularities inside BHs. The first true 3D simulation of spinning and moving BHs was performed in [7]. In [7], the two BHs start out very close to each other, closer than the separation for the last stable orbit, and the evolution proceeds through parts of the plunge and ring-down phase of a “grazing collision” within a very short time interval. The spacetime singularities are dealt with by a particular choice of coordinates, singularity avoiding slicing and vanishing shift.

BH excision [8,9] has allowed improvements in the treatment of the spacetime singularities to the extent that highly accurate simulations of single BHs can be carried out [10–14] and recent applications to the grazing collision of BHs show promise [15]. One of the key limiting factors in the existing two approaches to the grazing collision is the achievable evolution time for which useful numerical data can be obtained, which due to numerical problems has been limited to $7M$ in [7], and to about $9M$ – $15M$ in [15]. Here time is measured in units of the total “ADM” mass M of the system as opposed to using the bare mass m of one of the BHs.

In this paper we consider singularity avoiding slicing.

We combine the application of a series of recently developed and tested physics analysis tools and techniques with significant progress made in overcoming the problems mentioned above, including the use of much more stable formulations and much greater computer power. Early, preliminary results from this series of simulations have been presented in [16,17], but we now provide the first detailed physics analysis not possible previously.

We compute BH initial data of the puncture type [18], corresponding to two BHs in orbit about each other, with unequal masses, linear momentum, and individual spins on each BH. The construction of such data sets, which involves solving the non-linear elliptic Hamiltonian constraint equation numerically, is described in [18]. A detailed survey of a sequence of such data sets including various physical properties is discussed in [19]. In this paper we choose punctures for each BH on the y -axis at $\pm 1.5m$, masses $m_1 = 1.5m$ and $m_2 = m$, linear momenta $P_{1,2} = (\pm 2, 0, 0)m$, and spins $S_1 = (-1/2, 0, -1/2)m^2$ and $S_2 = (0, 1, -1)m^2$. Note that the linear momentum is perpendicular to the line connecting the BHs, equal but opposite for a vanishing net linear momentum, and that the spins are somewhat arbitrarily chosen to obtain a general configuration.

For this case, an asymptotic estimate for the initial ADM mass is $M = 3.22m$. Solving the Hamiltonian constraint leads to a larger value than the Brill-Lindquist mass of $m_1 + m_2 = 2.5m$. The angular momentum for puncture data is given by (independent of the solution to the Hamiltonian constraint) $\vec{J} = 2\vec{d}_1 \times \vec{P}_1 + \vec{S}_1 + \vec{S}_2$, where \vec{d}_1 is the vector from the origin to the first puncture. The total angular momentum is therefore $J = 7.58m^2$, which corresponds to an angular momentum parameter of $a/M = J/M^2 = 0.73$. In this configuration the individual spins increase the total angular momentum, so we call it the “high- J ” case. The following discussion refers

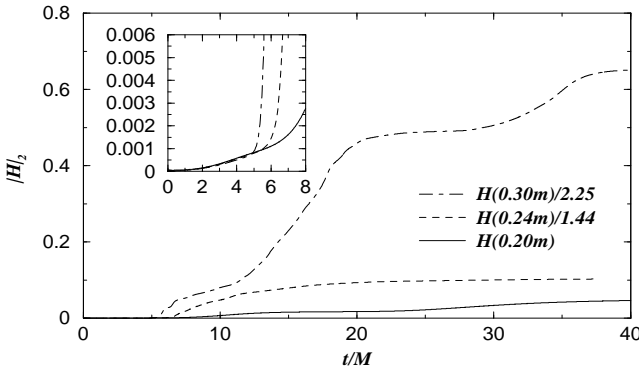


FIG. 1. Root-mean-square value of the Hamiltonian constraint on a centered cube with outer boundary at $38m$ and a gridspacing of $0.30m$, $0.24m$, $0.20m$. The curves are rescaled so that they coincide for second order convergence.

exclusively to this one data point in parameter space, except that when discussing waveforms below we compare the high-J case with data where the individual spins vanish (medium-J, $M = 3.00m$, $J = 6.00m^2$, $a/M = 0.67$) or where $S_1 \rightarrow -S_1$ and $S_2 \rightarrow -S_2$ (low-J, $M = 3.07m$, $J = 4.64m^2$, $a/M = 0.49$).

This initial data is evolved with evolution equations of the “BSSN” family [20,21], using the implementation that we developed and tested for the collapse of strong gravitational waves to BHs in [22]. We discuss some reasons why certain variable choices and certain combinations of the evolution equations with the constraints can lead to more stable evolutions than the traditional “ADM” system in [23], and we do observe a significant improvement in numerical stability in practice. We use radiative boundary conditions for the outer boundary. The coordinate singularities at the BH punctures are handled as in [7,11] by a time independent conformal factor. We solve the maximal slicing condition on the initial slice and then use the so-called 1+log slicing for the lapse and vanishing shift during the evolutions.

The computer simulations were carried out on a 3D cartesian grid. On a 256 processor SGI/Cray Origin 2000 machine at NCSA we were able to run simulations of 387^3 , which take roughly 100GB of memory (to our knowledge this makes them the largest production numerical relativity simulations to date). A good balance between resolution in the inner region and distance to the outer grid boundary was achieved for a grid spacing of $0.2m$, which puts the outer boundary for a centered cube at about $38m$ or about $12M$. All said, the combination of resolution, outer boundary location and treatment, coordinate choice, evolution system and puncture method for the BHs allows evolution times past $30M$. The lowest quasi-normal mode of the ring-down phase of the final rapid Kerr BH has a period of about $13M$ ($17M$ for Schwarzschild), therefore evolution times of $30M$ or more are a prerequisite for wave extraction, which was not pos-

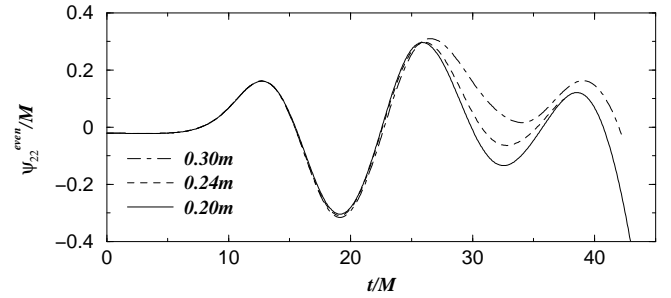


FIG. 2. Waveform at resolutions $0.30m$, $0.24m$, $0.20m$.

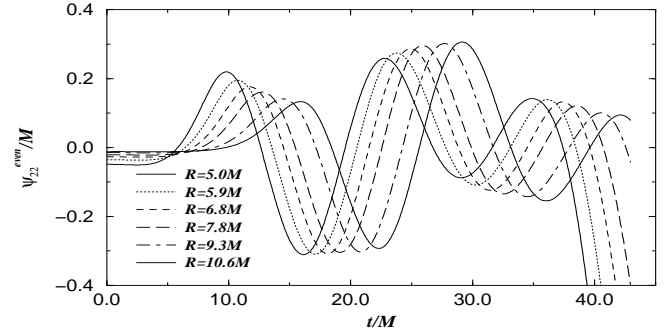


FIG. 3. Mode $l = m = 2$ of the even Zerilli function extracted for different radii as a function of time. A wave that develops after the BHs collide is propagating out.

sible in [7,15]. The simulations do not crash at that time, but as we will discuss now, the numerical data becomes degraded due to effects of the outer boundary and due to grid-stretching (i.e. large metric gradients) in the vicinity of the BHs. Fig. 1 shows the root-mean-square value of the Hamiltonian constraint over the entire grid for different resolutions but same outer boundary location. The inset shows clean global second order convergence up to about $6M$. A local analysis shows that there are large contributions to this average from inside the horizon, and that smaller errors intrude from the outer boundary, but the code is convergent beyond $30M$.

Since a main result of the simulations are waveforms,

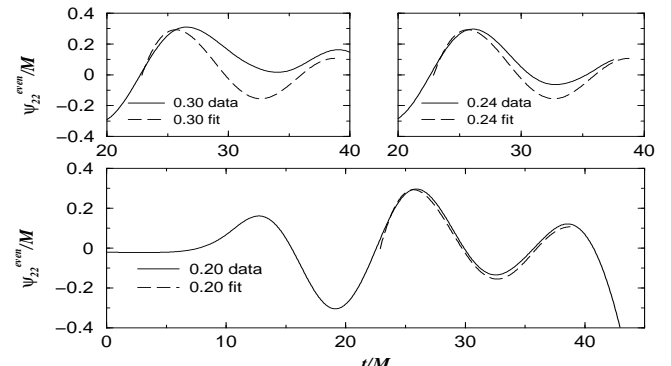


FIG. 4. A fit to the quasi normal mode determined by M and a shows good agreement in the frequency and decay rate at late times for a resolution of $0.2m$.

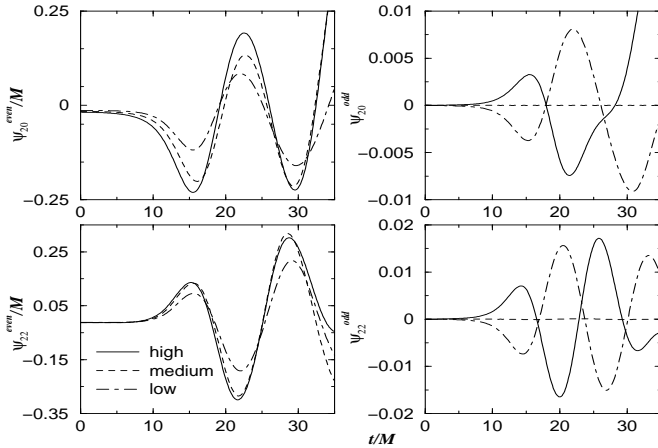


FIG. 5. Even and odd wave parts showing differences depending on high, medium, and low-J data.

the most relevant measure and often most stringent criterion for numerical quality is convergence in the waveforms. We use the gauge invariant waveform extraction technique, developed originally by Abrahams [24] and applied to the 3D case in [25], to extract gravitational wave modes of arbitrary ℓ, m . As shown in [25,26], this technique can be used on numerically evolved 3D distorted BH spacetimes to produce very accurate waveforms away from the BH, even if errors are rather large near the horizon. Here, we extract for example the nonaxisymmetric $\ell = m = 2$ mode, expected to be one of the most important modes in binary BH coalescence [27]. Fig. 2 shows for three resolutions the Zerilli function $\psi_{22}^{even}(t)$ extracted at $R = 7.8M$. Up to a time $t \approx 30M$ the dependence on resolution is rather small, which suggests that the resolution reaches the convergent regime.

In Fig. 3, we show a sequence of extracted waves at different radii, obtained by integration over the corresponding coordinate spheres, as a function of time. The outermost detectors show late time problems due to spurious signals propagating in from the outer boundary, while the inner detectors are affected by the closeness to the strong field region. Note that these methods assume a Schwarzschild background, but they can be applied on a rotating BH, the primary effect being an offset depending on the rotation parameter a [28]. In Fig. 4, we show the $l = m = 2$ even parity wave for the detector at $R = 7.8M$ and a match to the corresponding lowest quasi-normal mode plus the first overtone. The values for M and a determine the quasi-normal frequency, while the amplitude and the offset in time are fitted. The observed period is $13M$, which is consistent with a final distorted Kerr BH with $a/M = 0.73$. Gravitational waves carry away energy and momentum from the BHs. For the energy, we have $dE/dt = 1/(32\pi) \sum_{l=2}^{\infty} \sum_{m=-l}^l ((d\psi_{lm}^{even}/dt)^2 + (\psi_{lm}^{odd})^2)$. Integrating the $l = 2, 3, 4$ modes up to $t = 35M$, we find $\Delta E = 0.0323m \approx 1\%M$.

One of the potential insights from the detection of

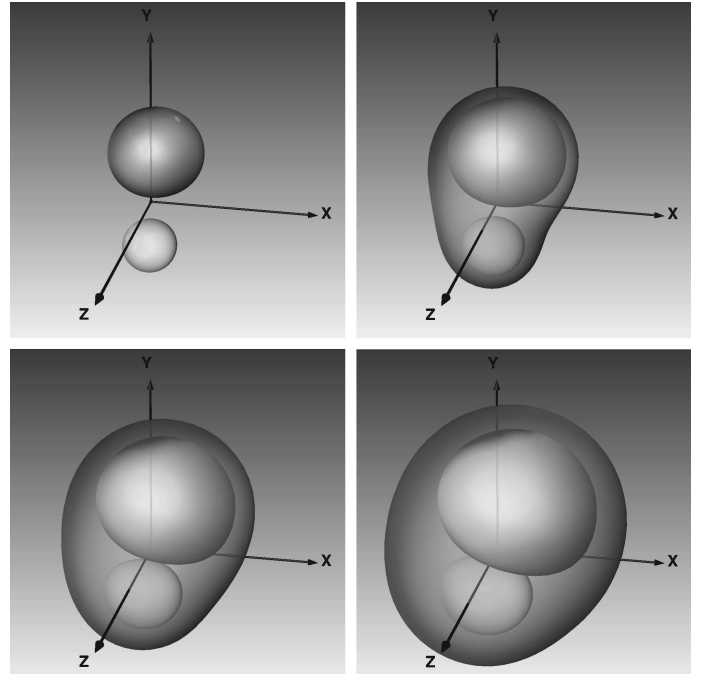


FIG. 6. The merger of the AH. Shown are marginally trapped surfaces at times $2.5M, 3.7M, 5.0M$, and $6.2M$. The apparent horizon is the outermost of these surfaces.

gravitational waves is the determination of the orientation of spins in relation to the orbital motion. Fig. 5 shows the wave signature for the high, medium, and low-J data. For vanishing spins (medium-J), we note that ψ_{20}^{odd} is zero within numerical accuracy, while ψ_{22}^{odd} shows an oscillation with amplitude 3×10^{-5} .

While it will be the waves that we can observe on earth directly, it is also interesting to compute the apparent horizon in the grazing BH collision. During the evolution we use a 3D apparent horizon (AH) finder described in [29] to track the location of the horizon. In principle, the event horizon can also be located by techniques developed in Ref. [30], but we do not yet know whether a single event horizon is present on the initial slice in this data set. Fig. 6 shows the AH during a grazing collision.

We compute the BH mass M_{AH} and compare with the ADM mass of the initial data and the radiated energy to assess the overall energy accounting. In Fig. 7, we show the result of the calculation of the so-called irreducible mass as a function of time, defined as $M_{ir} = \text{Area}_{AH}/(16\pi)$. The horizon mass M_{AH} can be determined through the formula $M_{AH}^2 = (M_{ir})^2 + J^2/(2M_{ir})^2$, where we use $J = 7.58m^2$ of the initial data. The observed upward drift in M_{ir} may be curable by excision or better coordinate conditions, but even in the present case we can estimate the final mass of the BH to be $M_{ir} \approx 3.0m$ and $M_{AH} \approx 3.3m$ in this simulation. Comparing this to the initial ADM mass of the spacetime, $M = 3.22m$, we find consistency in the overall energy accounting from independent physical measurements. The

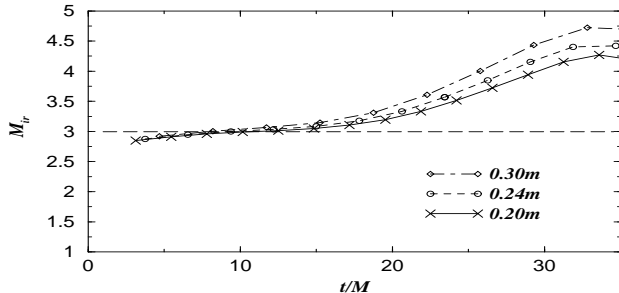


FIG. 7. We show the evolution of M_{ir} for the high-J configuration. As the BHs merge, the area grows, and then begins to level, as the final BH goes into the ringdown. But numerical error associated with the grid stretching effects causes a spurious growth in the area, familiar in previous 2D and 3D studies. However, one can estimate the mass of the final BH, as shown by the dashed line.

fraction of the total energy, 1%, that is carried away in the gravitational waves falls within the error estimate of this energy balance.

In conclusion, these results indicate that for the first time we are indeed able to simulate the late merger stages of two BHs colliding, with rather general spin, mass, and momenta, and that we can begin to examine the fine details of the physics. Studies of apparent horizons, waveforms, and asymptotic properties show consistency in the analysis across strong field, near zone, and far field regions. Without more advanced techniques, such as BH excision, these simulations will be limited to the final merger phase of BH coalescence. But while that is under development, we can take advantage of our capabilities and explore this phase of the inspiral now. Our goal is several fold: (a) to explore new BH physics of the “final plunge” phase of the binary BH merger, (b) to try to determine some useful information relevant for gravitational wave astronomy, and (c) to provide a strong foundation of knowledge for this process that will be useful when more advanced techniques are fully developed. A new development is the Lazarus project, which provides an interface between full numerical relativity simulations and perturbative evolutions [31], and an interface to the post-Newtonian inspiral phase is planned. At this time Lazarus allows us to move a finite time interval of full numerical evolution into the early stages of the merger, and to perform the ring-down calculation efficiently once the final BH enters the perturbative regime. When these techniques and excision are used to extend the ability of the community to handle the collision of two BHs starting from the late orbital phase, it will be important to have an understanding of details of the most violent merger phase in advance, both as a testbed to ensure that results are correct, and because the understanding we gain may be useful in devising the appropriate techniques for longer term evolution.

Acknowledgments. We thank in particular G. Allen,

J. Baker, M. Campanelli, T. Goodale, C. Lousto, and many colleagues at the AEI, Washington University, Universitat de les Illes Balears, and NCSA for the co-development of the Cactus code, and for important discussions and assistance. Calculations were performed at AEI, NCSA, SDSC, RZG, and ZIB.

- [1] B. Schutz, gr-qc/9911034 (1999).
- [2] L. Smarr, Ann. N. Y. Acad. Sci. **302**, 569 (1977).
- [3] S. L. Shapiro and S. A. Teukolsky, Phys. Rev. D **45**, 2739 (1992).
- [4] P. Anninos *et al.*, Phys. Rev. Lett. **71**, 2851 (1993).
- [5] P. Anninos *et al.*, Phys. Rev. D **52**, 2044 (1995).
- [6] R. Matzner *et al.*, Science **270**, 941 (1995).
- [7] B. Brügmann, Int. J. Mod. Phys. D **8**, 85 (1999).
- [8] J. Thornburg, Classical and Quantum Gravity **4**, 1119 (1987).
- [9] E. Seidel and W.-M. Suen, Phys. Rev. Lett. **69**, 1845 (1992).
- [10] P. Anninos *et al.*, Phys. Rev. D **51**, 5562 (1995).
- [11] P. Anninos *et al.*, Phys. Rev. D **52**, 2059 (1995).
- [12] G. B. Cook *et al.*, Phys. Rev. Lett. **80**, 2512 (1998).
- [13] R. Gomez *et al.*, Phys. Rev. Lett. **80**, 3915 (1998), gr-qc/9801069.
- [14] M. Alcubierre and B. Brügmann, (2000), preprint.
- [15] S. Brandt *et al.*, submitted, gr-qc/0009047.
- [16] E. Seidel, in *Proceedings of the Yukawa Conference* (PUBLISHIER, Kyoto, Japan, 1999).
- [17] B. Brügmann, Ann. Phys. (Leipzig) **9**, 227 (2000), gr-qc/9912009.
- [18] S. Brandt and B. Brügmann, Phys. Rev. Lett. **78**, 3606 (1997).
- [19] L. Nerger, Master’s thesis, Universität Bremen, 2000.
- [20] T. W. Baumgarte and S. L. Shapiro, Physical Review D **59**, 024007 (1999).
- [21] M. Shibata and T. Nakamura, Phys. Rev. D **52**, 5428 (1995).
- [22] M. Alcubierre *et al.*, Phys. Rev. D **61**, 041501 (2000), gr-qc/9904013.
- [23] M. Alcubierre *et al.*, (1999), gr-qc/9908079.
- [24] A. Abrahams, Ph.D. thesis, University of Illinois, Urbana, Illinois, 1988.
- [25] G. Allen, K. Camarda, and E. Seidel, (1998), gr-qc/9806036, submitted to Phys. Rev. D.
- [26] J. Baker *et al.*, Phys. Rev. D **62**, 127701 (2000), gr-qc/9911017.
- [27] Éanna É. Flanagan and S. A. Hughes, Phys. Rev. D **57**, 4535 (1998), gr-qc/9701039.
- [28] S. Brandt and E. Seidel, Phys. Rev. D **52**, 870 (1995).
- [29] M. Alcubierre *et al.*, (1998), gr-qc/9809004. To appear in Class. Quant. Grav.
- [30] P. Anninos *et al.*, Phys. Rev. Lett. **74**, 630 (1995).
- [31] J. Baker, B. Brügmann, M. Campanelli, and C. O. Lousto, Class. Quant. Grav. **17**, L149 (2000), gr-qc/0003027.